Effective collision frequency due to ion-acoustic instability: Theory and simulations

Petr Hellinger and Pavel Trávníček

Institute of Atmospheric Physics, AS CR, Prague, Czech Republic

J. Douglas Menietti

University of Iowa, USA

We study the ion-acoustic instability driven by a drift between Maxwellian protons and electrons in a nonmagnetized plasma using a Vlasov simulation with the realistic proton to electron mass ratio. Simulation results for similar electron and proton temperatures are in good agreement with predictions. Namely, during the linear and saturation phases the effective collision frequency observed in the simulation is in quantitative agreement with the quasi-linear predictions. However, previous estimates [*Galeev and Sagdeev*, 1984; *Labelle and Treumann*, 1988] give the effective collision frequency less than one tenth the simulated values. The theoretical and simulation results are in a partial agreement with the simulation work by *Watt et al.* [2002] who used a non-realistic mass ratio. After the saturation, the effective collision frequency increases owing to the existence of backward-propagating ion-acoustic waves. These waves result from induced scattering on protons and contribute to the anomalous transport of electrons.

1. Introduction

Current driven instabilities play an important role in the dissipation and field-line merging in shocks and reconnection regions in collisionless plasma. Recent works [*Watt et al.*, 2002; *Petkaki et al.*, 2003] indicate that the ion-acoustic instability (in a nonmagnetized plasma) driven by a drift velocity between protons and electrons is more important than was previously thought [*Labelle and Treumann*, 1988]. Theoretical works [*Galeev and Sagdeev*, 1984; *Labelle and Treumann*, 1988] give an estimate for the second order effects, the effective collision frequency $\nu = |dp_e/dt|/p_e$ (where p_e is electron momentum) of the ion-acoustic instability in the case of cold protons in an analogue form to the classical Spitzer (electron-ion) collision frequency:

$$\nu \sim \omega_{pe} \frac{W_e}{n k_B T_e}, \tag{1}$$

where ω_{pe} is the electron plasma frequency, W_e is the fluctuating ion-acoustic wave energy, n is the electron density, k_B is Boltzmann constant, and T_e is the electron temperature. Recently, *Watt et al.* [2002] performed a set of Vlasov simulations and measured the effective collision frequency ν in the simulations and found values two to three orders of magnitude higher than those predicted by Equation (1). The simulation work by *Watt et al.* [2002] indicates that Equation (1) is not applicable for a plasma with comparable proton and electron temperatures. However, the interesting and probably important results of *Watt et al.* [2002] have a major drawback: These simulations were done for an artificial proton to electron mass ratio $m_p/m_e = 25$.

This paper addresses the question of the effective collision frequency resulting from the ion-acoustic drift instability using a Vlasov simulation with realistic mass ratio $m_p/m_e = 1836$ for these parameters: proton to electron temperature ratio $T_p/T_e = 0.5$ and drift velocity between electrons and protons $v_d = 1.7 v_{the}$ (v_{the} is the electron thermal velocity). Note, that we have chosen the same parameters as used by *Watt et al.* [2002]. The paper is organized as follows: First, in section 2 we present an overview of the linear and quasi-linear theory of ion-acoustic drift instability. Then, in section 3 we describe the simulation method and in section 4 we show results of the simulation and compare them with the theoretical predictions of section 2. Finally, in section 5 we discuss the results.

2. Linear and Quasi-linear Theory

We investigate the properties of a plasma with proton and electron populations with Maxwellian distribution functions, drifting with respect to each other, $f_p = n/((2\pi)^{1/2} v_{thp}) \exp(-v^2/(2v_{thp}^2))$, and $f_e = n/((2\pi)^{1/2} v_{the}) \exp(-(v - v_d)^2/(2v_{the}^2))$, respectively, where n is the plasma density, v_d is the drift velocity, v_{thp} is the proton thermal velocities.

For a drift velocity v_d of the order of electron thermal velocity v_{the} the system is unstable with respect to the ion-acoustic instability. The growth of ion-acoustic waves leads in the second order to slowing down of electrons $dp_e/dt < 0$. The second order, quasi-linear effect for a spectrum $\delta E(k)$ of the ion-acoustic waves may be given in a similar manner as for the lower-hybrid drift instability [*Davidson and Gladd*, 1975] as:

$$\frac{dp_e}{dt} = \int dk |\delta E(k)|^2 \frac{\omega_{pe}^2}{k v_{the}^2} \text{Im} \xi_e Z(\xi_e) \tag{2}$$

where $\xi_e = (\omega - k v_d)/(\sqrt{2} k v_{the})$ and Z is the plasma dispersion function. The dispersion relation $\omega = \omega(k)$ is given in a standard way

$$1 + \frac{\omega_{pe}^2}{k^2 v_{the}^2}(1 + \xi_e Z(\xi_e)) + \frac{\omega_{pp}^2}{k^2 v_{thp}^2}(1 + \xi_p Z(\xi_p)) = 0, \tag{3}$$

where ω_{pp} is the proton plasma frequency and $\xi_p = \omega/(\sqrt{2} k v_{thp})$. Equations (3) and (2) hold as long as the distribution functions of electrons and protons are not far away from the initial Maxwellian distributions.

3. Code

For integration of the one-dimensional Vlasov-Poisson system of equations we use a slightly modified version [*Mangeney et al.*, 2002] of the Vlasov code developed by *Fijalkow* [1999]. The code has periodic boundary conditions and uses a Fourier transform for the integration of the Poisson equation.

The electron and proton distribution function f_e and f_p are discretized both in space and in velocities. The spatial grid has $N_x = 16,384$ points and a resolution $\Delta x = 1/8\lambda_D$ (λ_D is the Debye length). The electron velocity grid has $N_{ve} = 2000$ points with the resolution $\Delta v_e = 0.01 v_{the}$, and minimum and maximum velocities are $v_{emin} = -8.3 v_{the}$ and $v_{emax} = 11.7 v_{the}$. Similarly, the proton velocity grid has $N_{vp} = 1000$ points with the resolution $\Delta v_p = 0.02 v_{thp}$ and minimum and maximum velocities are $v_{pmin} = -10 v_{thp}$ and $v_{pmax} = 10 v_{thp}$.

4. Simulation Results

We initialize the simulation with a proton and electron Maxwellian distribution with the physical parameters $v_d = 1.7 v_{the}$ and $T_p/T_e = 0.5$ [cf. *Watt et al.*, 2002]. For these parameters Equation (3) predicts that the ion-acoustic branch is unstable for a wide range of wave vectors (from nearly zero to about $0.85/\lambda_D$) with the maximum growth rate $\gamma_{max} = 0.00632\omega_{pe}$, for the wave vector $k_{max} = 0.51/\lambda_D$ and frequency $\omega = 0.0158\omega_{pe}$. Since the Vlasov simulations are essentially noiseless, we add to the initial distribution functions f_e and f_p seed fluctuations δf_e and δf_p that correspond to a linear response of the distribution function to small, random phase fluctuating electric field $E = \delta E \sum_k \exp(ikx - \omega t + \phi)$ of the ion-acoustic waves:

$$\delta f_{e,p} = \mp \frac{e}{m_{e,p}} \mathrm{Re} \sum_k \frac{E \exp(ikx - \omega t + \phi(k))}{i(kv - \omega)} \frac{\partial f_{e,p}}{\partial v} \quad (4)$$

where $\omega = \omega(k)$ is a solution of the linear dispersion equation (3) and $\phi = \phi(k)$ is a random number from 0 to 2π. We have chosen $\delta E = 5 \times 10^{-7} m_e v_{the}\omega_{pe}/e$ and the initial spectrum of wave vectors in Equation (4) to lie between $0.04/\lambda_D$ and $1/\lambda_D$, i.e. mainly in the unstable region.

We let the simulation evolve from the initial seed at time $t = 0$ to the final time $t = 4000$ (henceforth the time is given in units of ω_{pe}^{-1}). During the simulation the electron and proton total mass are conserved with a precision 10^{-7} whereas the total energy is conserved with a precision 10^{-4}. The evolution of the simulated system may be divided into three phases: First, the waves grow exponentially, then they saturate in a quasi-linear manner, and fi-

nally, after saturation the fluctuating electric field decreases through wave-wave and wave-particle interactions.
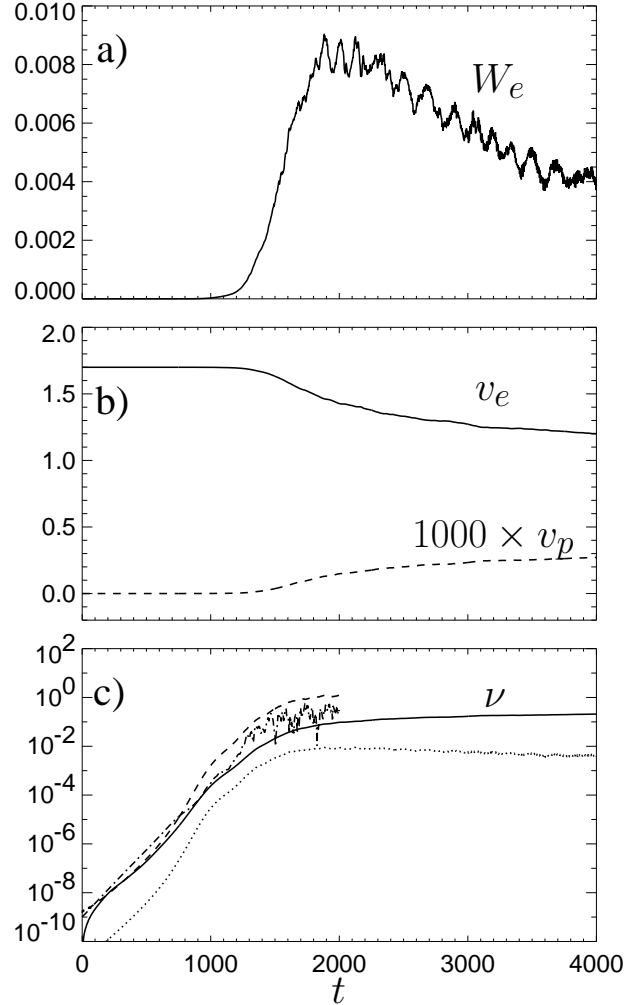

Figure 1. Evolution of (a) the fluctuating electric field energy W_e, (b) the mean electron (solid) and proton (dashed) velocities v_e and v_p, respectively, and (c) the effective collision frequency ν: The solid curve shows the value measured in the simulation via Equation (5), the dashed and dash-dotted denote the estimates of Equations (6) and (7), respectively. The prediction based on Equation (1) is shown by the dotted curve.

Figure 1 shows an evolution of different quantities during the simulation: Figure 1a displays evolution of the density of fluctuating electric field energy $W_e = \langle \epsilon_0 \delta E^2 \rangle/(2nk_B T_e)$ where $\langle \delta E^2 \rangle = \sum_{i=1}^{N_x} \delta E_i^2/N_x$. Figure 1b shows evolution of electron and proton mean velocities v_e and v_p denoted by solid and dashed curve, respectively. Finally, Figure 1c (solid curve) displays the effective collision frequency ν measured in the simulation as

$$\nu(t + \delta t/2) = \frac{2}{\delta t} \frac{p(t + \delta t) - p(t)}{p(t + \delta t) + p(t)} \quad (5)$$

where we use $\delta t = 1$. The dashed and dash-dotted curves show theoretical prediction of the the effective collision frequency ν calculated from the quasi-linear theory using the simulated spectrum $\delta E(k)$ and linear dispersion predictions of Equation (3): The dashed curve shows an estimate based on the discrete version of

Equation (2):

$$\nu = \sum_k \frac{\Delta k |\delta E(k)|^2 \omega_{pe}^2}{k v_{the}^2 m_e n v_d} \mathrm{Im}\, \xi_e Z(\xi_e) \qquad (6)$$

and the dash-dotted curve shows an estimate calculated using only the strongest unstable mode from Equation (6) [cf. *Davidson and Gladd*, 1975]:

$$\nu = \frac{|\delta E(k_{\max})|^2 \omega_{pe}^2}{k_{\max} v_{the}^2 m_e n v_d} \mathrm{Im}\, \xi_e Z(\xi_e). \qquad (7)$$

The dotted curve shows the estimate of Equation (1).

Figure 1a shows clearly three phases: First an exponential growth and a saturation about the time $t = 2000$, and, later on, a decay of fluctuating wave energy W_e. In the post-saturation phase there are small oscillations in the fluctuating energy W_e with a frequency $\omega_E = 0.05\omega_{pe}$ indicating possible electron trapping. An estimation of the trapping frequency in a monochromatic wave with wave vector k and an amplitude δE_k based on a lowest order approximation gives $\omega_b = (ek|\delta E_k|/m)^{1/2}$. The strongest mode in the simulation at the saturation level ($t = 2000$) would give a value of ω_b about ten times greater than the observed frequency ω_E. The oscillation of the fluctuating energy W_e is probably due to other effects.

Figure 1b displays the coupling between the protons and electrons owing to the instability; electrons are decelerated whereas protons are slightly accelerated. The electron deceleration takes place all through the simulation, and is more pronounced for a stronger fluctuating electric field as expected from the quasi-linear theory (Equation (2)). This deceleration translates into the effective collision frequency ν. Figure 1c shows that the observed frequency ν is in a very good agreement with the theoretical predictions of the quasi-linear theory, especially during the first linear stage $t \lesssim 600$ but around the saturation the simulated value is about one tenth the quasi-linear prediction. On the other hand, Equation (1) predicts almost two orders of magnitude lower values for $t \lesssim 600$ and about one order lower values around the saturation.

The saturation value $\nu \sim 0.1\omega_{pe}$ is below the values predicted by Equations (6) and (7) as one may expect: If only quasi-linear effects are present, the evolution of the averaged distribution function $\bar{f}_e(v)$ would be governed by a quasi-linear diffusion

$$\frac{\partial \bar{f}_e}{\partial t} = \frac{\partial}{\partial v}\left(D \frac{\partial \bar{f}_e}{\partial v}\right) \qquad (8)$$

with the diffusion coefficient D, and the electron distribution function would eventually become stationary $\partial \bar{f}_e/\partial t = 0$ with a quasi-linear plateau in the resonant region $\partial \bar{f}_e/\partial v = 0$. Consequently, the effective collision frequency $\nu = |dp_e/dt|/p_e$ would eventually approach zero. However, in the simulation ν continues to increase from approximately 0.1 to 0.2 even after the saturation whereas the amplitude of electric fluctuation $|\delta E|^2$ decreases. This result indicates the presence of other effects playing important role in the third, post-saturation phase. Let us now investigate the evolution of the simulated system in detail.

The simulated system is initially dominated by the unstable ion-acoustic waves, and, later on, back-propagating ion-acoustic waves appear. There is a negligible wave energy in the Langmuir branch since the initial seed (Equation (4)) was given to the unstable ion-acoustic branch and the Vlasov simulations are essentially noiseless. The simulated spectra are shown in Figure 2. Figure 2 displays the fluctuating electric field δE as a function of ω and k as gray scale plots in two time intervals: (a) the initial, linear phase ($t = 0$–800) and (b) the post-saturation phase ($t = 2000$–4000). Overplotted curves denote predictions of the linear theory, Equa-

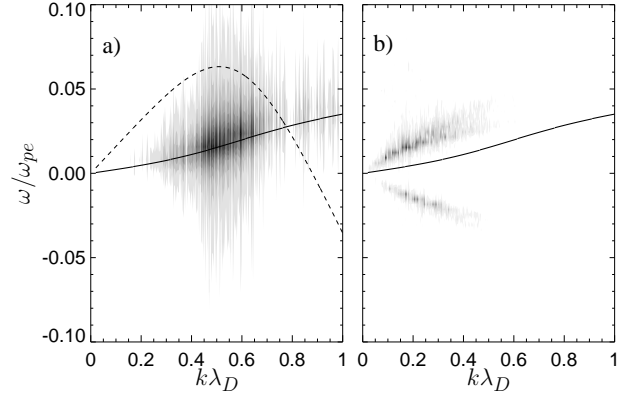tion (3): Solid and dashed curves show the frequency and ten times the growth rate, respectively.

Figure 2. Gray scale plots of simulated spectra: Fluctuating electric field δE as a function of ω and k during (a) initial linear phase and (b) post-saturation phase. Overplotted curves denote predictions of the linear theory: Solid and dashed curves show the frequency and ten times the growth rate, respectively.

Figure 2a shows that initially the ion-acoustic waves are generated with the dispersion predicted by the linear theory (solid line) and in the unstable region (dashed line). Later on, Figure 2b the dispersion of the initially unstable waves is strongly modified and, moreover, back-propagating ion-acoustic waves appear.

The change of the dispersion (the increase of phase velocity, see Figure 2b), is related to the quasi-linear heating of the electrons since the ion-acoustic velocity is proportional to the thermal velocity of electrons. The electron distribution function indeed clearly exhibits a signature of important heating as documented in Figure 3. Figure 3 displays reduced distribution functions of (a) electrons $f_e = f_e(v)$ and (b) protons $f_p = f_p(v)$ at different times (dotted curves) $t = 0$, (dashed curves) $t = 2000$, and (solid curves) $t = 4000$ (see Figure 1). Note, that for protons we use a logarithmic scale. Figure 3a indeed shows that at around the saturation, $t = 2000$ (dashed curve), the electron distribution function strongly departs from the initial drift Maxwellian one (dotted curve). At the end of the simulation the electron distribution function is dominated by a pronounced plateau (solid curve) which extends also to the negative velocities. This effect is a direct consequence of the presence of back-propagating ion-acoustic waves. Concerning the proton distribution function, Figure 3b shows that, that only strongly suprathermal protons (with about $|v| > 5v_{thp}$) are accelerated.

Combining the results we got so far we have an explanation of the growth of the effective collision frequency ν (Figure 1c) after the saturation. This effect is related to the appearance of back-propagating ion-acoustic waves. These back-propagating ion-acoustic waves heat electrons and extend the quasi-linear plateau to negative electron velocities (see Figure 3a) which leads to the increase of ν. These waves probably result from an induced scattering of the instability-generated ion-acoustic waves on protons: The core part of the proton distribution satisfies the condition of the wave-wave-particle interaction $(k_1 - k_2)v = \omega_1 - \omega_2$ between forward (k_1, ω_1) and backward (k_2, ω_2) propagating ion acoustic waves (note that we suppose $\omega_{1,2} > 0$, $k_1 > 0$, and $k_2 < 0$ in contrast with Figure 2). The oscillation of the fluctuating electric field energy W_e (see Figure 1) may be connected with the back-propagating waves. The beating of forward and backward propagating waves would yield a frequency comparable to the observed frequency ω_E.
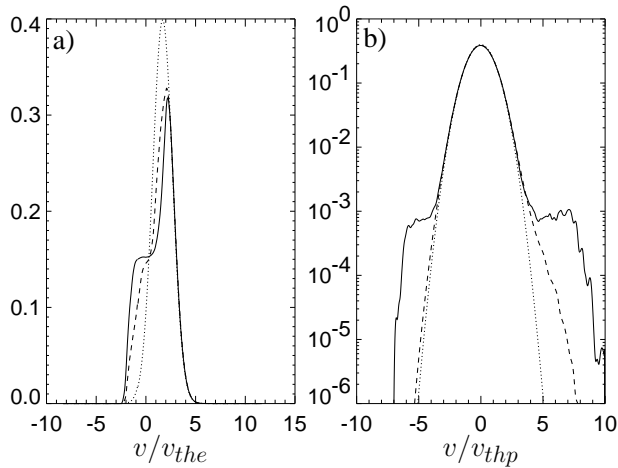
Figure 3. Reduced distribution function of (a) electrons $f_e(v)$ and (b) protons $f_p(v)$ at different times (dotted curves) $t = 0$, (dashed curves) $t = 2000$, and (solid curves) $t = 4000$ (see Figure 1). Note, that for protons we use logarithmic scale.

5. Discussion

In this paper we have presented linear and quasi-linear theory of the ion-acoustic drift instability and compared these theoretical predictions with Vlasov simulations in the case of these initial plasma parameters [the same parameters as in *Watt et al.*, 2002]: The temperature ratio $T_p/T_e = 0.5$ and the drift velocity between electrons and protons $v_d = 1.7v_{the}$.

The simulation results are in quantitative and qualitative agreement with the predictions of linear and quasi-linear theory [*Davidson and Gladd*, 1975]. Namely, the effective collision frequency $\nu = |dp_e/dt|/p_e$ observed in the simulation is very close to the values predicted from the quasi-linear theory during the linear phase and even around the saturation. The electrons are slowed down even after the saturation owing to the appearance of back-propagating ion-acoustic waves. These waves are likely produced by induced scattering on protons as discussed by *Galeev and Sagdeev* [1984]. A quantitative comparison with these theoretical predictions is beyond the scope of this paper. The back-propagating ion-acoustic waves interacts with electrons and extends the plateau to negative electron velocities, so that the electrons are slowed down and the effective collision frequency increases after the saturation.

The effective collision frequency observed in the simulation is from about two orders (during the linear phase) to one order of magnitude (around the saturation) greater than the estimations of Equation (1). This difference is considerably smaller than the results of *Watt et al.* [2002] which is likely owing to the fact that *Watt et al.* [2002] used the non-realistic mass ratio since the effective collision frequency scales as $m_e/m_p^{1/2}$ [*Petkaki et al.*, 2003]. Further investigation of this problem is beyond the scope of this paper.

The disagreement between the simulations and estimation of Equation (1) is not surprising since these estimations [*Galeev and Sagdeev*, 1984] are derived for $T_p \ll T_e$ and for three-dimensional geometry whereas in our simulation [and in those by *Watt et al.*, 2002] there is $T_p/T_e = 0.5$ and the physics is constrained to one spatial and one velocity dimensions. Future work will be devoted to the study of the influence of the initial plasma parameters and the impact of a second spatial dimension.

References

Davidson, R. C., and N. T. Gladd (1975), Anomalous transport properties associated with the lower-hybrid-drift instability, *Phys. Fluids*, *18*, 1327–1335.

Fijalkow, E. (1999), Numerical solution to the Vlasov equation: the 1D code, *Comp. Phys. Comm.*, *116*, 329–335.

Galeev, A. A., and R. Z. Sagdeev (1984), Current instabilities and anomalous resistivity in plasma, in *Handbook of Plasma Physics, Basic Plasma Physics*, vol. II, edited by A. A. Galeev and R. N. Sudan, pp. 271–303, North-Holland, Amsterdam.

Labelle, J., and R. A. Treumann (1988), Plasma waves at the dayside magnetopause, *Space Sci. Rev.*, *47*, 175–202.

Mangeney, A., F. Califano, C. Cavazzoni, and P. Trávníček (2002), A numerical scheme for the integration of the Vlasov-Maxwell system of equations, *J. Comput. Phys.*, *179*, 495–538.

Petkaki, P., C. E. J. Watt, R. B. Horne, and M. P. Freeman (2003), Anomalous resistivity in non-Maxwelian plasmas, *J. Geophys. Res.*, *108*, 1442, doi:10.1029/2003JA010092.

Watt, C. E. J., R. B. Horne, and M. P. Freeman (2002), Ion-acoustic resistivity in plasmas with similar ion and electron temperatures, *Geophys. Res. Lett.*, *29*, 1004, doi:10.1029/2001GL013451.

P. Hellinger and P. Trávníček Institute of Atmospheric Physics, AS CR, Prague 14131, Czech Republic. (Petr.Hellinger@ufa.cas.cz; trav@alenka.ufa.cas.cz)

J. D. Menietti, Department of Physics and Astronomy, University of Iowa, USA (jdm@space.physics.uiowa.edu)